RM L51L27

NACA RM L51L27

NACA

# RESEARCH MEMORANDUM

## TRANSONIC FLIGHT TESTS TO COMPARE THE ZERO-LIFT DRAGS OF 45° SWEPTBACK WINGS OF ASPECT RATIO 3.55 AND 6.0 WITH AND WITHOUT NACELLES AT THE WING TIPS

By Sherwood Hoffman and Richard C. Mapp, Jr.

Langley Aeronautical Laboratory
Langley Field, Va.

NATIONAL ADVISORY COMMITTEE FOR AERONAUTICS

WASHINGTON
March 6, 1952

NATIONAL ADVISORY COMMITTEE FOR AERONAUTICS

---

RESEARCH MEMORANDUM

---

# TRANSONIC FLIGHT TESTS TO COMPARE THE ZERO-LIFT DRAGS OF 45° SWEPTBACK WINGS OF ASPECT RATIO 3.55 AND 6.0 WITH AND WITHOUT NACELLES AT THE WING TIPS

By Sherwood Hoffman and Richard C. Mapp, Jr.

## SUMMARY

Rocket-propelled models were flight-tested at transonic speeds to compare the zero-lift drags of 45° sweptback wings having aspect ratios of 3.55 and 6.0 with and without solid nacelles at the wing tips. The aspect-ratio-3.55 wing was derived by removing 35.5 percent of the semispan from the outboard part of the aspect-ratio-6.0 wing. The fuselage and nacelle fineness ratios were 10.0 and 9.66, respectively. The wings had the NACA 65A009 airfoil section in the free-stream direction.

The wing drag coefficient was lowered at high subsonic and supersonic speeds when the aspect ratio was reduced from 6.0 to 3.55. Near a Mach number of 1.0, decreasing the aspect ratio increased the wing drag coefficient. The wing-tip nacelle locations on both the high- and low-aspect-ratio wings were favorable from a drag standpoint; however, less favorable nacelle-plus-interference drag was obtained at the wing tip by reducing the span of the high-aspect-ratio wing. The force-break Mach number of the configuration was reduced from 0.96 to 0.93 by removing 35.5 percent of the semispan from the aspect-ratio-6.0 wing.

## INTRODUCTION

As part of a general transonic research program of the National Advisory Committee for Aeronautics to investigate the aerodynamic properties of promising aircraft configurations, the Langley Pilotless Aircraft Research Division (at its testing station at Wallops Island, Va.) has tested several rocket-propelled free-flight models to determine the effect of nacelle location on the zero-lift drags of transonic research configurations. Previous investigations (references 1, 2, 3, and 4) show the variations of drag coefficient with Mach number for a configuration having a high-aspect-ratio, 45° sweptback wing with solid nacelles located in several chordwise, spanwise, and vertical positions on the wing. Because of the low drag obtained when nacelles were located at the wing tip (reference 3), especially near a Mach number of 1.0, the wing-tip location was selected for further investigation. The present paper gives a comparison of the zero-lift drags of 45° sweptback wings having aspect ratios of 3.55 and 6.0 with and without nacelles mounted at the wing tips.

The nacelles were proportioned to house an axial-flow turbojet engine with an afterburner. The basic lines of the nacelle nose were designed to accommodate NACA 1-series nose inlets with critical Mach numbers above 0.90.

To simplify this investigation, the nacelles were made solid by fairing the nose inlet to a point. Reference 5 shows that the variation of drag with Mach number at a mass-flow ratio of about 0.7 for the ducted nacelles was approximately the same as the drag from the solid nacelles located in corresponding positions at the wing tips.

The flight tests covered a continuous Reynolds number range from $3.8 \times 10^6$ at a Mach number of 0.8 to $7.6 \times 10^6$ at a Mach number of 1.25.

## SYMBOLS

| | |
|---|---|
| $A$ | aspect ratio $\left(b^2/S_W\right)$ |
| $a$ | tangential acceleration, feet per second per second |
| $b$ | wing span, feet |
| $C_D$ | total drag coefficient, based on $S_W$ |
| $C_{D_N}$ | drag coefficient for nacelle-plus-interference drag, based on $S_F$ |
| $C_{D_{W_e}}$ | drag coefficient for wing, based on $S_{W_e}$ |
| $g$ | acceleration due to gravity, 32.2 feet per second per second |
| $M$ | Mach number |

$q$ free-stream dynamic pressure, pounds per square foot

$R$ Reynolds number, based on wing mean aerodynamic chord

$S_F$ frontal area of one nacelle, square feet

$S_W$ total wing plan-form area, square feet

$S_{W_e}$ exposed wing plan-form area, square feet

$W$ model weight during deceleration, pounds

$\gamma$ angle between flight path and horizontal, degrees

## MODELS

Details and dimensions of the wing-body-fin combinations, the solid nacelle, and the nacelle positions are given in figures 1, 2, and 3. Coordinates of the fuselage, airfoil section, and nacelle are given in reference 1. Photographs showing the general arrangements of the models tested are presented in figure 4.

The two wings used for the drag comparisons of this investigation were sweptback 45° along the quarter-chord line and had the NACA 65A009 airfoil section in the free-stream direction. The wing of aspect ratio 6.0 (fig. 1) was used in the previous nacelle investigations (references 1 to 6) and is referred to, for convenience, as the original wing. The wing of aspect ratio 3.55, which is tested in this investigation, was derived from the original wing by clipping off 35.5 percent of the semispan from the outboard part of the original wing. The taper ratios of the clipped wing and the original wing were 0.75 and 0.6, respectively.

The fuselage had a fineness ratio of 10.0. The ratio of total wing plan-form area to body frontal area was 10.6 for the clipped wing configuration and 16.0 for the original configuration. The leading edges of both wings tested intersected the fuselage contour at the maximum-diameter station.

Each nacelle was a solid body of revolution having an NACA 1-50-250 nose-inlet profile, a cylindrical midsection, and an afterbody having the proportions of form 111 of reference 7. The inlet was faried to a point, making the nacelle solid. The fineness ratio of the solid nacelle was 9.66.

The wing-tip nacelle location of the clipped wing model corresponded to the 60-percent-semispan nacelle location of the original wing (model E, fig. 3(c)) with the outboard part of the wing removed. The center lines of the nacelles were located in the wing plane parallel to the free-stream direction. The noses of the nacelles were located at a constant distance ahead of the wing maximum thickness as is shown in figure 3.

## TESTS AND MEASUREMENTS

The rocket-propelled zero-lift models were tested at the Langley Pilotless Aircraft Research station, Wallops Island, Va. Reference 8 gives a detailed description of the rocket-testing method and instrumentation used for this investigation. Velocity and trajectory data were obtained from the CW Doppler velocimeter and the NACA modified SCR584 tracking radar unit. A survey of atmospheric conditions for each test was made through radiosonde measurements from an ascending balloon.

The flight tests covered a continuous Mach number range from 0.8 to 1.25. The Reynolds number, based on wing mean aerodynamic chord, varied from $3.8 \times 10^6$ to $7.6 \times 10^6$ over the test range as is shown in figure 5.

Values of total drag coefficient, based on total wing-plan-form area, were calculated for decelerating flight with the relationship

$$C_D = -\frac{W}{qgS_W}(a + g \sin \gamma)$$

The variations of wing drag coefficient with Mach number were obtained by subtracting the drag of the body and two fins (reference 6) from the drags of the wing-body combinations tested. The wing drag coefficient based on exposed wing area of each wing tested is

$$C_{D_{W_e}} = \left(C_{D_{wing\text{-}body}} - C_{D_{body}}\right)\frac{S_W}{S_{W_e}}$$

where $C_{D_{wing\text{-}body}}$ and $C_{D_{body}}$ are based on $S_W$.

The variations of nacelle-plus-interference drag coefficient with Mach number were obtained from the difference in drag coefficient of faired $C_D$ curves of a model with nacelles and a model without nacelles. This coefficient based on nacelle frontal area is

$$C_{D_N} = \left(C_{D_{nacelles\ on}} - C_{D_{nacelles\ off}}\right)\frac{S_W}{2S_F}$$

where $C_{D_{nacelles\ on}}$ and $C_{D_{nacelles\ off}}$ are based on $S_W$.

The magnitude of the error in drag coefficient was established from the test results of three identical models without nacelles in reference 1 and was based on the maximum deviation found between curves faried through the experimental points. At flight Mach numbers from 0.8 to 0.93 and 1.02 to 1.25, the errors in total drag coefficient (based on $S_W$ of clipped wing), wing drag coefficient (based on $S_{W_e}$ of clipped wing), nacelle-plus-interference drag coefficient, and Mach number are believed to be within the following limits:

$C_D$ . . . . . . . . . . . . . . . . . . . . . . . . . . . . $\pm 0.0006$

$C_{D_{W_e}}$ . . . . . . . . . . . . . . . . . . . . . . . . . . $\pm 0.001$

$C_{D_N}$ . . . . . . . . . . . . . . . . . . . . . . . . . . $\pm 0.05$

$M$ . . . . . . . . . . . . . . . . . . . . . . . . . . . . $\pm 0.005$

Because the slope of the drag curve changes rapidly near Mach number 1.0, the errors in drag coefficient are larger than in the foregoing table. For a Mach number error of about $\pm 0.01$ at transonic speeds, the errors in drag coefficient are believed to be less than the following:

$C_D$ . . . . . . . . . . . . . . . . . . . . . . . . . . . . $\pm 0.0025$

$C_{D_{W_e}}$ . . . . . . . . . . . . . . . . . . . . . . . . . . $\pm 0.006$

$C_{D_N}$ . . . . . . . . . . . . . . . . . . . . . . . . . . $\pm 0.1$

## RESULTS AND DISCUSSION

The variations of total drag coefficient with Mach number for the clipped-wing models without nacelles (model A) and with nacelles (model B) are given in figure 6. The variation of $C_D$ with $M$ for the isolated nacelles in figure 6 and reference 1 was estimated from theoretical and experimental data of noses and afterbodies and includes boundary-layer effects by adding the drag coefficients of a parabolic nose, a cylindrical midsection, and a boattail at various Mach numbers through the test range. A comparison of the drag curves shows that the subsonic drag coefficient of the two flight models was about equal up to a Mach number of 0.91. At Mach numbers from 0.92 to 1.25, the experimental drag from the nacelles was slightly less than the estimated drag of the isolated nacelles.

In order to compare the drags of the configurations having the clipped wings, the original wings (references 3 and 6), and no wings (reference 6), the values of $C_D$ in figure 7(a) were based on the total wing area of the original wing. From the variations of $C_D$ with $M$ for all the models, it is evident that reducing the wing area of the original wing lowered the total drag through most of the speed range. A comparison of the wing-body drags (models A and C) with the drag of the body alone (model F) shows that the wing drag was reduced considerably at supersonic speeds (about 50 percent at $M = 1.25$) by clipping off 35.5 percent of the semispan from the outboard part of the original wing.

Figure 7(b) shows that the wing drag coefficient was lowered at high subsonic and supersonic speeds by reducing the aspect ratio of the wing from 6.0 to 3.55. Allowing for changes in wing drag due to wing-body interference, the variations of wing drag coefficient with Mach number at supersonic speeds in figure 7(b) agree with the theoretical predictions of reference 9. From these predictions, decreasing the aspect ratio of sweptback wings at low supersonic speeds where the Mach line is well in front of the wing leading edge increases the wing drag coefficient. At supersonic speeds where the Mach line approaches the wing leading edge, $C_{D_{W_e}}$ decreases with decreasing aspect ratio. The same effects of aspect ratio and Mach number on $C_{D_{W_e}}$ as shown in figure 7(b) were obtained for 45° sweptback wings of high and low aspect ratio in reference 10.

It is shown in reference 3 and figure 7(a) that adding nacelles to the wing tips of the aspect-ratio-6.0 wing (model D) reduced the total drag of the original wing-body configuration (model C) near Mach number 1.0. From a comparison of the nacelle-plus-interference drags in figure 7(c) for the wing-tip locations on the high- and low-aspect-ratio wings with that estimated for isolated nacelles, it is evident that the wing-tip nacelle location on both wings is favorable from a drag standpoint; however, less favorable nacelle interference is obtained at the wing tip of the aspect-ratio-3.55 wing than at the tip of the aspect-ratio-6.0 wing.

Model E, which is the configuration used in deriving the clipped-wing model with nacelles, had the greatest total drag (fig. 7(a)) and nacelle-plus-interference drag throughout the speed range, especially near Mach number 1.0. In figure 7(c), the results indicate that the large nacelle-plus-interference drag from model E at transonic speeds was due to unfavorable interference between the nacelle and the wing. This unfavorable interference was reduced considerably by removing that part of the original wing between the nacelle and wing tip.

The force-break Mach number of the configuration was reduced from 0.96 to 0.93 by removing 35.5 percent of the semispan from the aspect-ratio-6.0 wing.

## CONCLUSIONS

The effect of aspect ratio and wing span on the zero-lift drag at transonic speeds of a 45° sweptback wing-body configuration with and without nacelles at the wing tips has been determined through flight tests from a Mach number of 0.8 to 1.25. The aspect ratio of the wing was reduced from 6.0 to 3.55 by removing 35.5 percent of the semispan. The following effects were noted:

1. The wing-drag coefficient was lowered at high subsonic and supersonic speeds when the aspect ratio was reduced from 6.0 to 3.55. Near a Mach number of 1.0, decreasing the aspect ratio increased the wing drag coefficient.

2. In general, the wing-tip nacelle locations were favorable from a drag standpoint; however, less favorable nacelle-plus-interference drag was obtained for the wing-tip nacelle location when the span of the wing was reduced.

3. The force-break Mach number of the configuration was reduced from 0.96 to 0.93 by removing 35.5 percent of the semispan from the outboard part of the aspect-ratio-6.0 wing.

Langley Aeronautical Laboratory
National Advisory Committee for Aeronautics
Langley Field, Va.

REFERENCES


1. Pepper, William B., Jr., and Hoffman, Sherwood: Transonic Flight Tests to Compare the Zero-Lift Drag of Underslung and Symmetrical Nacelles Varied Chordwise at 40 Percent Semispan of a 45° Sweptback, Tapered Wing. NACA RM L50G17a, 1950.

2. Pepper, William B., Jr., and Hoffman, Sherwood: Comparison of Zero-Lift Drags Determined by Flight Tests at Transonic Speeds of Symmetrically Mounted Nacelles in Various Chordwise Positions at the Wing Tip of a 45° Sweptback Wing and Body Combination. NACA RM L51F13, 1951.

3. Pepper, William B., Jr., and Hoffman, Sherwood: Comparison of Zero-Lift Drags Determined by Flight Tests at Transonic Speeds of Symmetrically Mounted Nacelles in Various Spanwise Positions on a 45° Sweptback Wing and Body Combination. NACA RM L51D06, 1951.

4. Hoffman, Sherwood: Comparison of Zero-Lift Drag Determined by Flight Tests at Transonic Speeds of Pylon, Underslung, and Symmetrically Mounted Nacelles at 40 Percent Semispan of a 45° Sweptback Wing and Body Combination. NACA RM L51D26, 1951.

5. Hoffman, Sherwood, and Pepper, William B., Jr.: Transonic Flight Tests to Determine Zero-Lift Drag and Pressure Recovery of Nacelles Located at the Wing Tips on a 45° Sweptback Wing and Body Combination. NACA RM L51K02, 1951.

6. Pepper, William B.: The Effect on Zero-Lift Drag of an Indented Fuselage or a Thickened Wing-Root Modification to a 45° Sweptback Wing-Body Configuration as Determined by Flight Tests at Transonic Speeds. NACA RM L51F15, 1951.

7. Abbott, Ira H.: Fuselage-Drag Tests in the Variable-Density Wind Tunnel: Streamline Bodies of Revolution, Fineness Ratio of 5. NACA TN 614, 1937.

8. Hoffman, Sherwood: Transonic Flight Tests to Compare the Drag at Zero-Lift of Nacelles Located in Various Positions on the Wing of a Sweptback Wing and Body Configuration. Univ. Va. Thesis, 1951.

9. Harmon, Sidney M.: Theoretical Supersonic Wave Drag of Untapered Sweptback and Rectangular Wings at Zero Lift. NACA TN 1449, 1947.

10. Mathews, Charles W., and Thompson, Jim Rogers: Drag Measurements at Transonic Speeds of NACA 65-009 Airfoils Mounted on a Freely Falling Body to Determine the Effects of Sweepback and Aspect Ratio. NACA RM L6K08c, 1947.

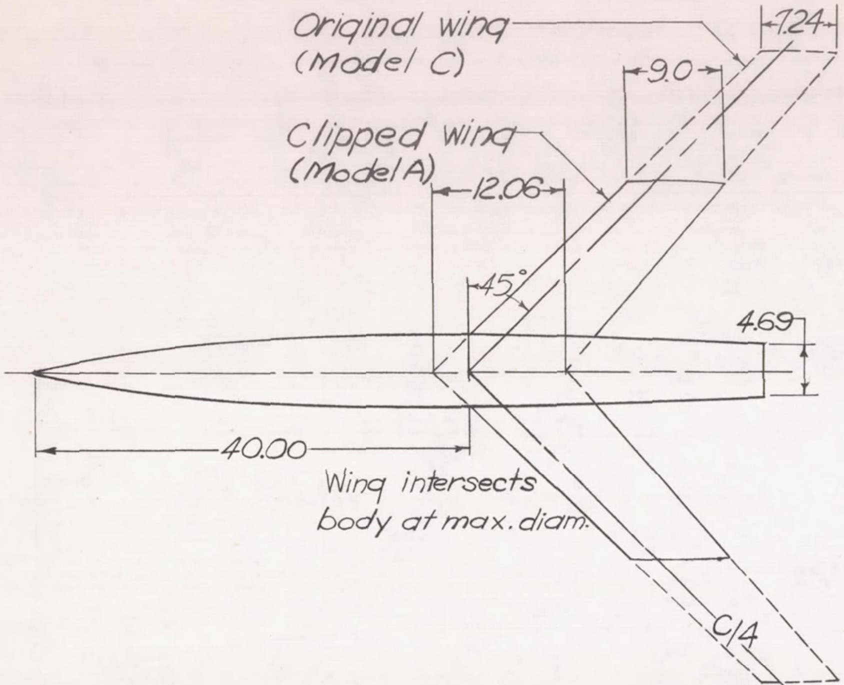


**Model Characteristics**

| | |
|---|---|
| Fuselage | |
| Fineness ratio | 10.0 |
| Frontal area, square feet | 0.243 |
| Clipped wing | |
| Aspect ratio | 3.55 |
| Taper ratio | 0.75 |
| Mean aerodynamic chord, feet | 0.886 |
| Airfoil parallel to free stream | NACA 65A009 |
| Total wing planform area, square feet | 2.722 |
| Exposed wing planform area, square feet | 2.177 |
| Original wing | |
| Aspect ratio | 6.0 |
| Taper ratio | 0.6 |
| Mean aerodynamic chord, feet | 0.822 |
| Airfoil parallel to free stream | NACA 65A009 |
| Total wing planform area, square feet | 3.878 |
| Exposed wing planform area, square feet | 3.333 |
| Fins | |
| Exposed fin planform area (2 fins), square feet | 0.468 |

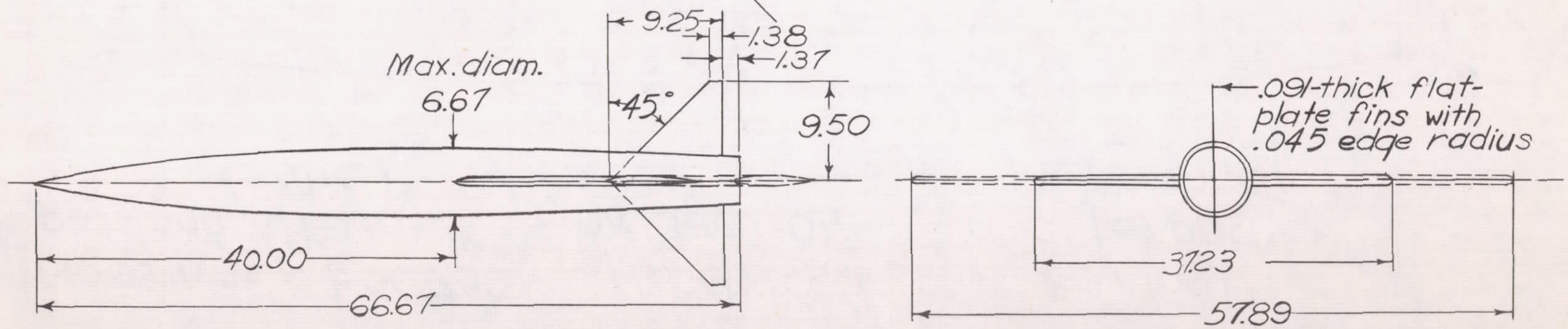


Figure 1.- General arrangement and dimensions of test model. All dimensions are in inches.

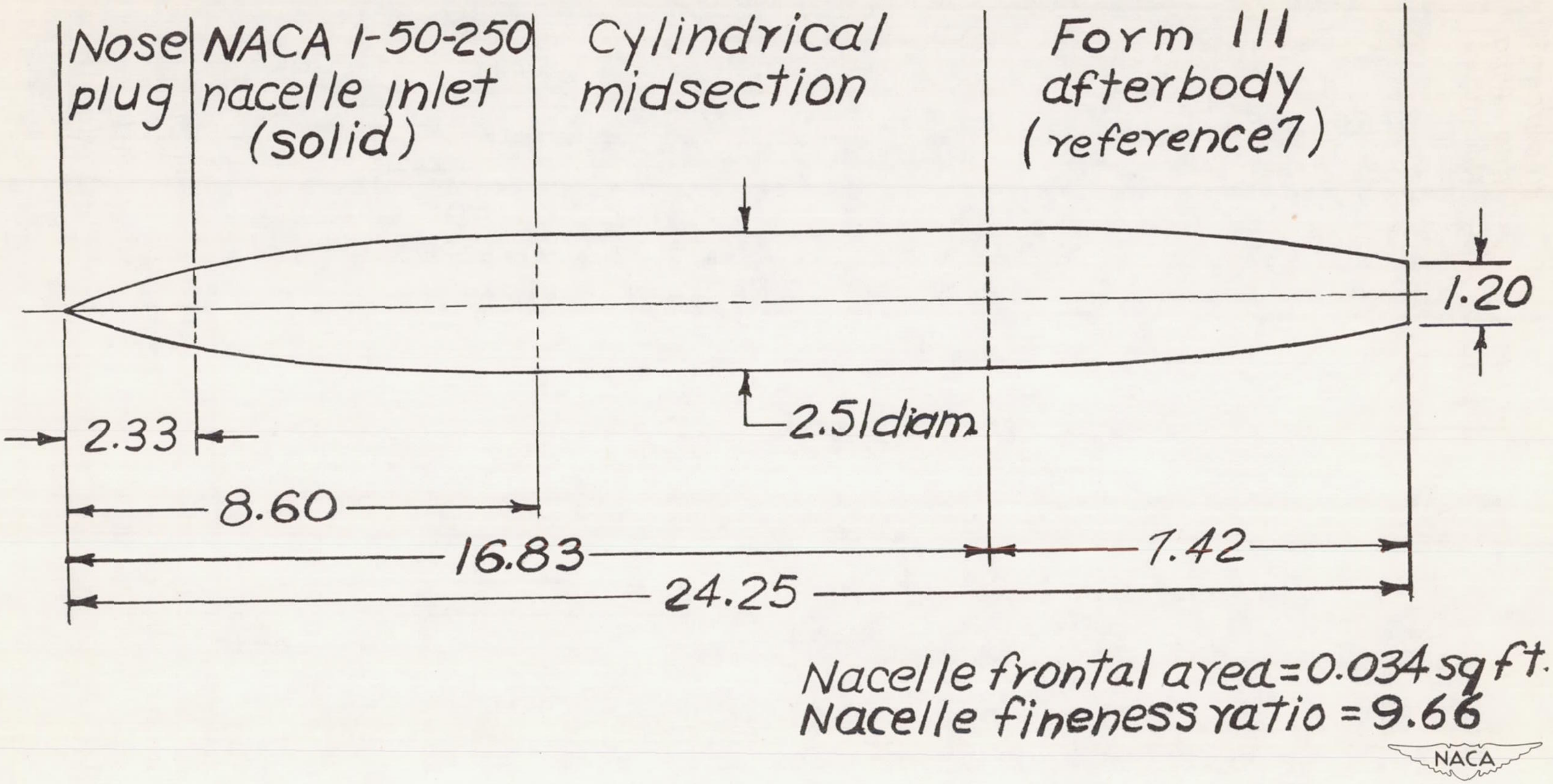


Figure 2.- Details and dimensions of nacelle. All dimensions are in inches.

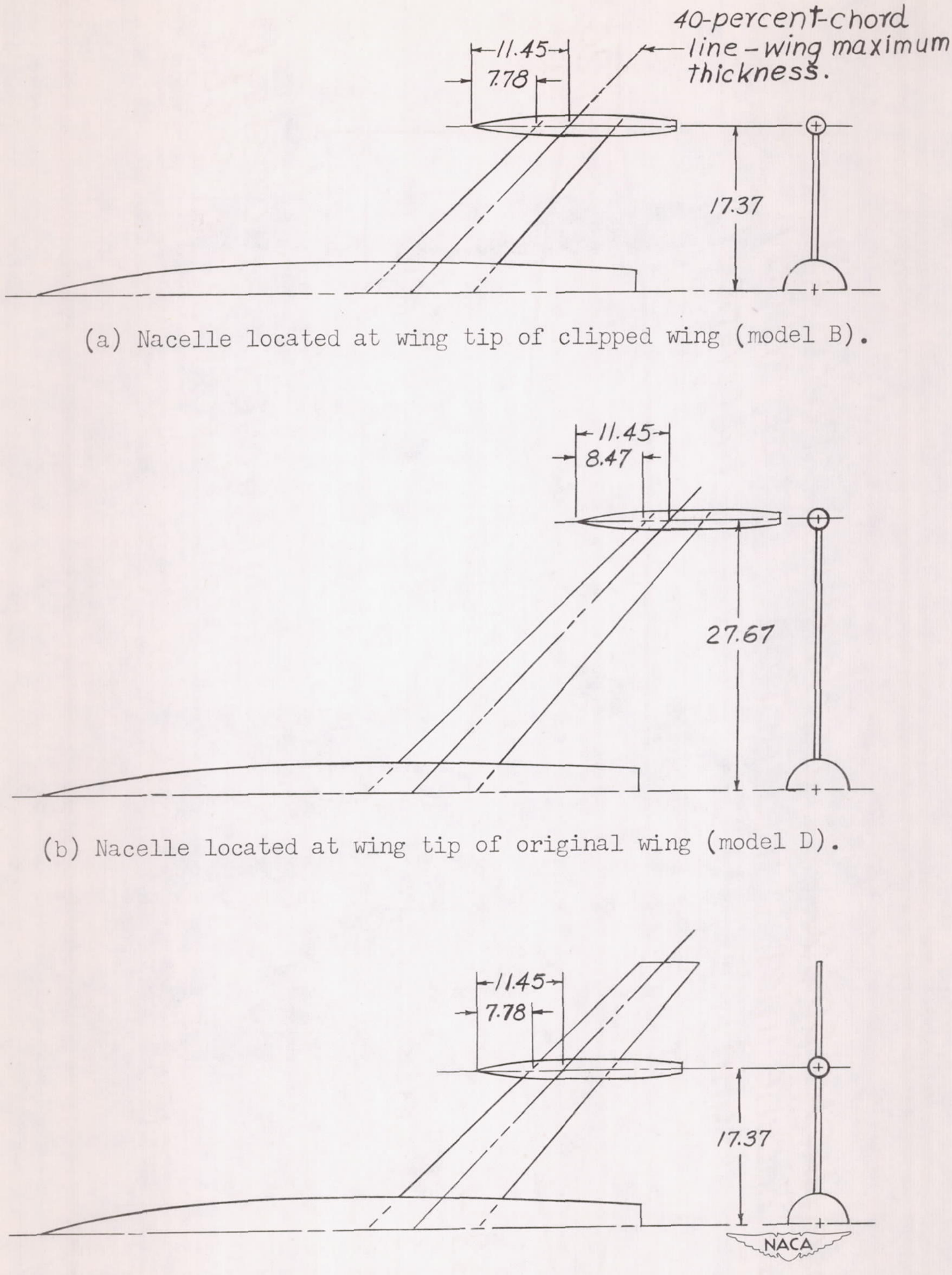


(a) Nacelle located at wing tip of clipped wing (model B).



(b) Nacelle located at wing tip of original wing (model D).



(c) Nacelle located at 60 percent semispan of original wing (model E).

Figure 3.- Comparison of nacelle locations on models. All dimensions are in inches.

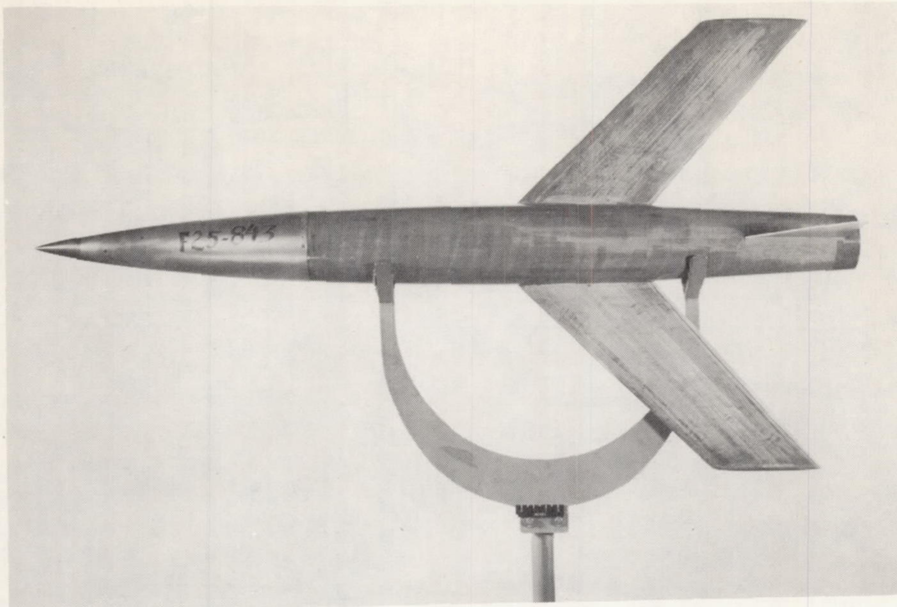

Model A

NACA
L-70133

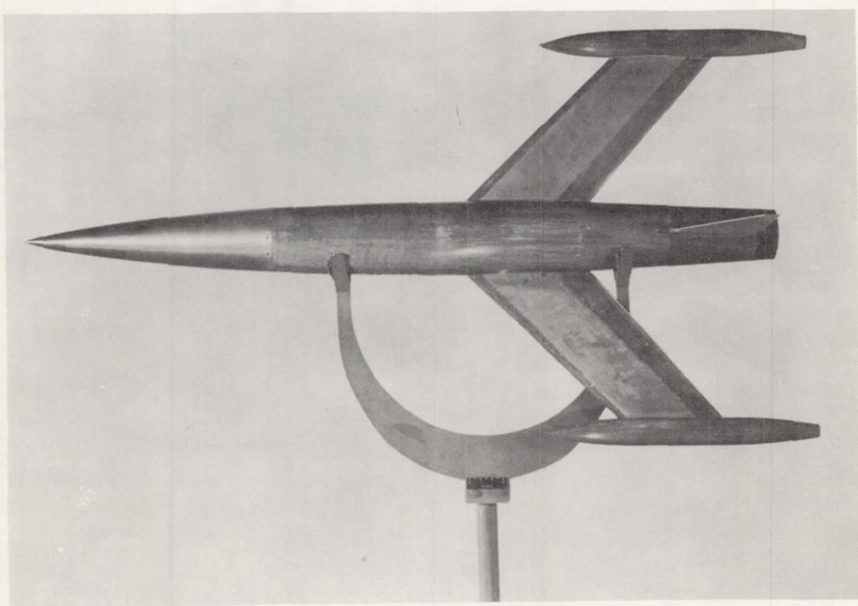

Model B

NACA
L-70275

(a) Models with aspect-ratio-3.55 wing.

Figure 4.- Photographs showing test models.

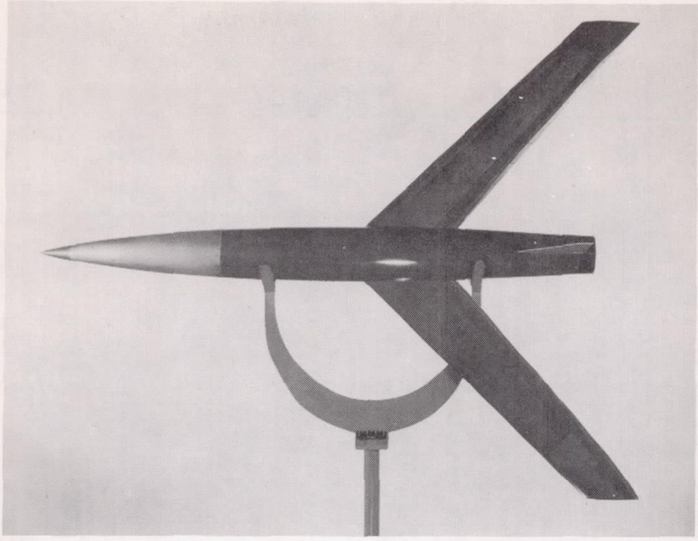

Model C

L-71869

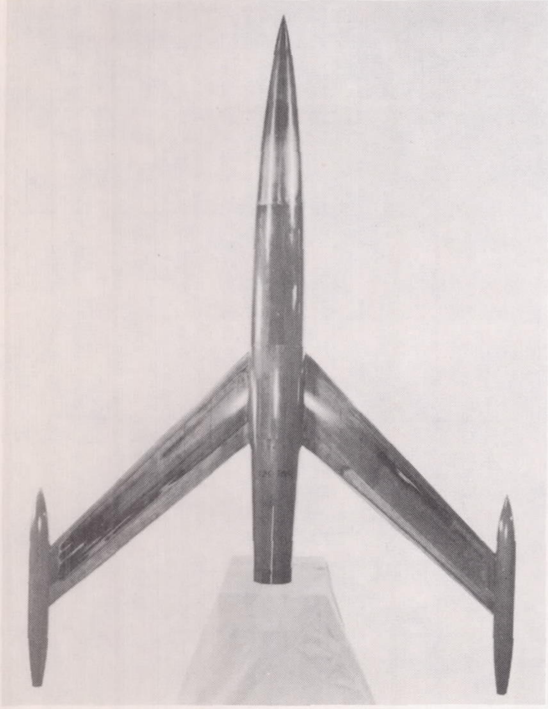

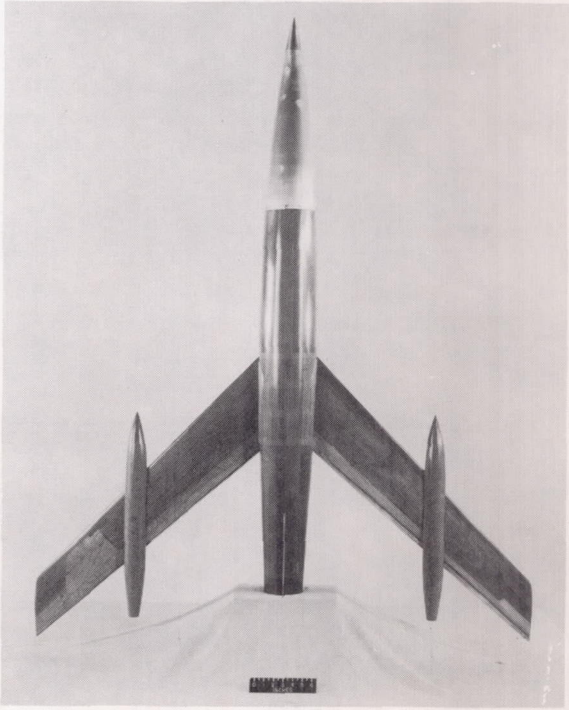

Model D

Model E

L-67572

(b) Models with aspect-ratio-6.0 wing.

L-65144

Figure 4.- Concluded.

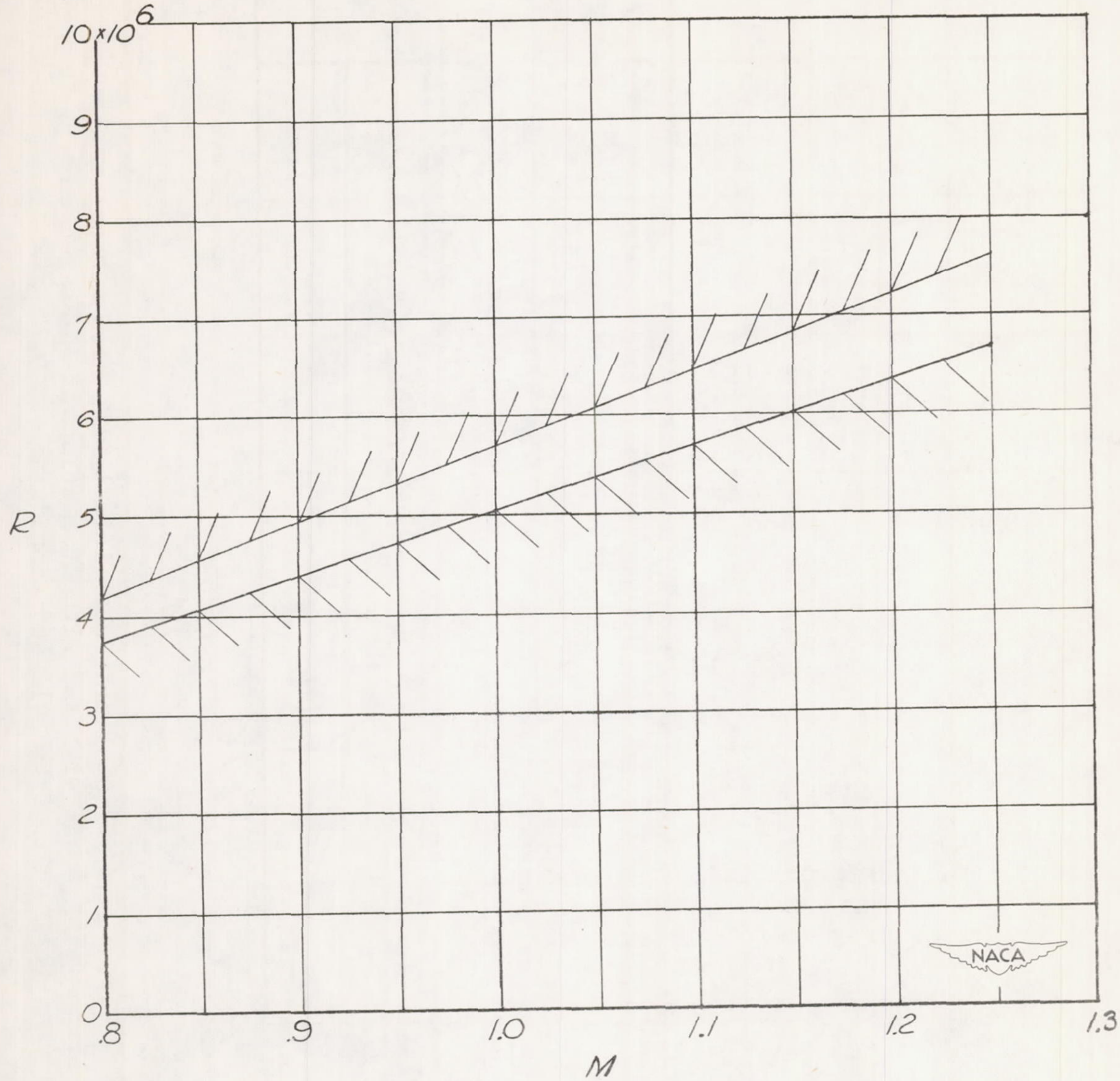


Figure 5.- Variation of Reynolds number with Mach number for all the models tested. Reynolds number based on wing mean aerodynamic chord.

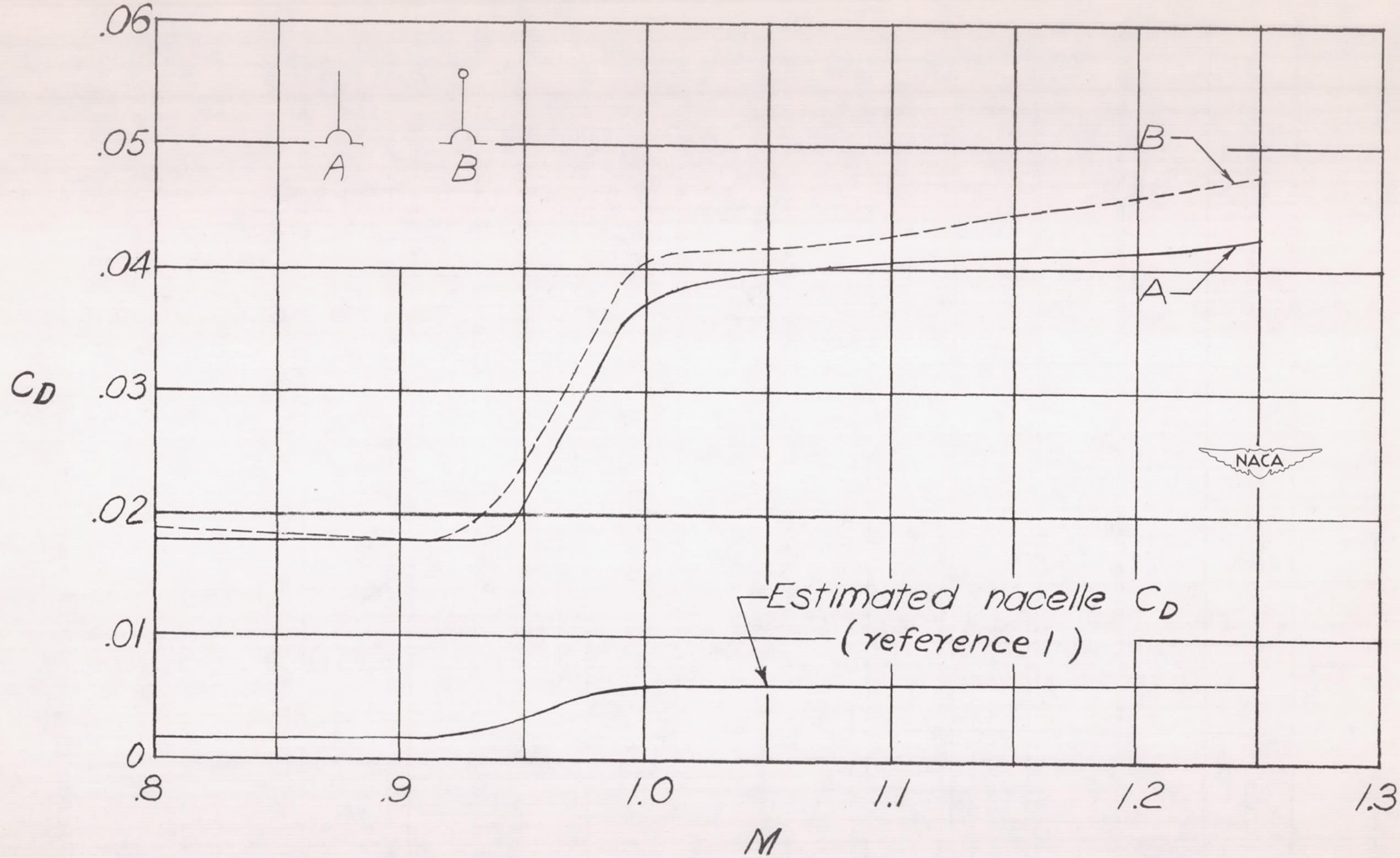


Figure 6.- Variations of total drag coefficient with Mach number for the clipped wing model with and without nacelles. $C_D$ based on total plan-form area of the clipped wing.

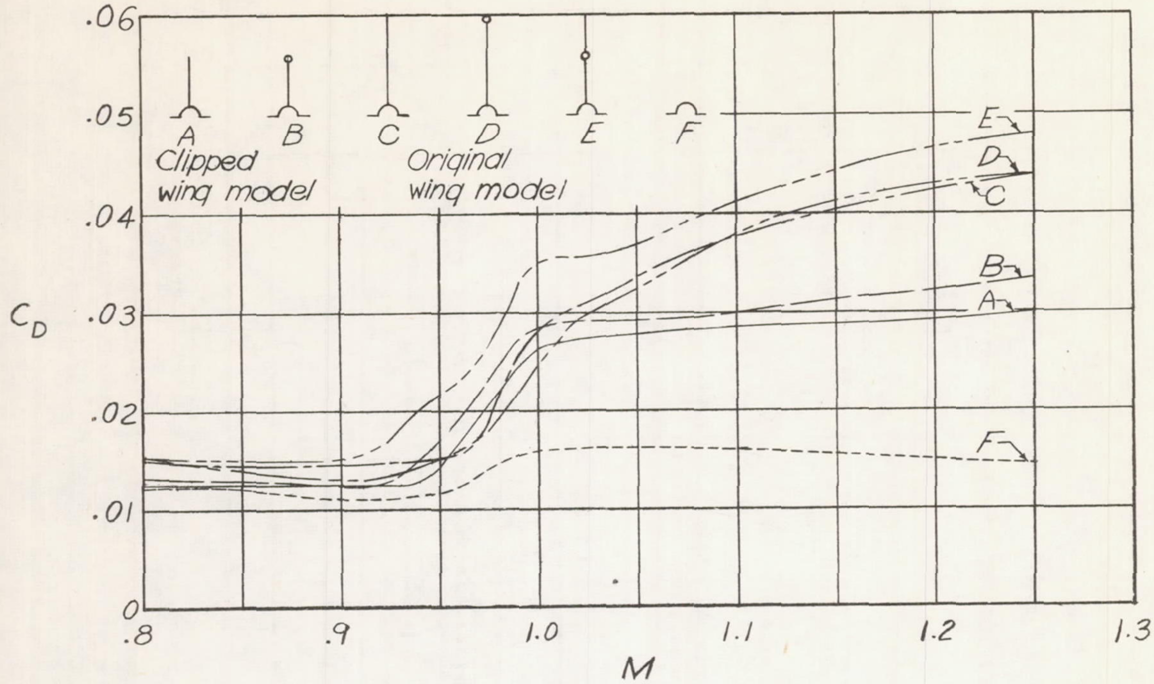


(a) Variation of total drag coefficient with Mach number. $C_D$ based on total plan-form area of original wing.

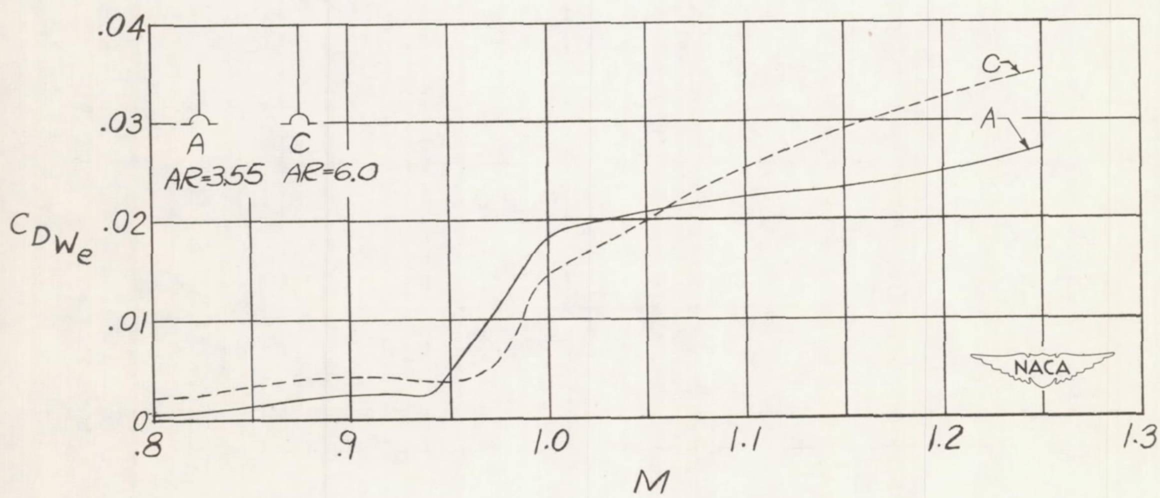


(b) Variation of wing drag coefficient with Mach number. $C_{D_{W_e}}$ based on exposed wing area of each wing.

Figure 7.- Comparison of total drag, wing drag, and nacelle-plus-interference drag coefficients at transonic Mach numbers for the models having the clipped wing and the original wing.

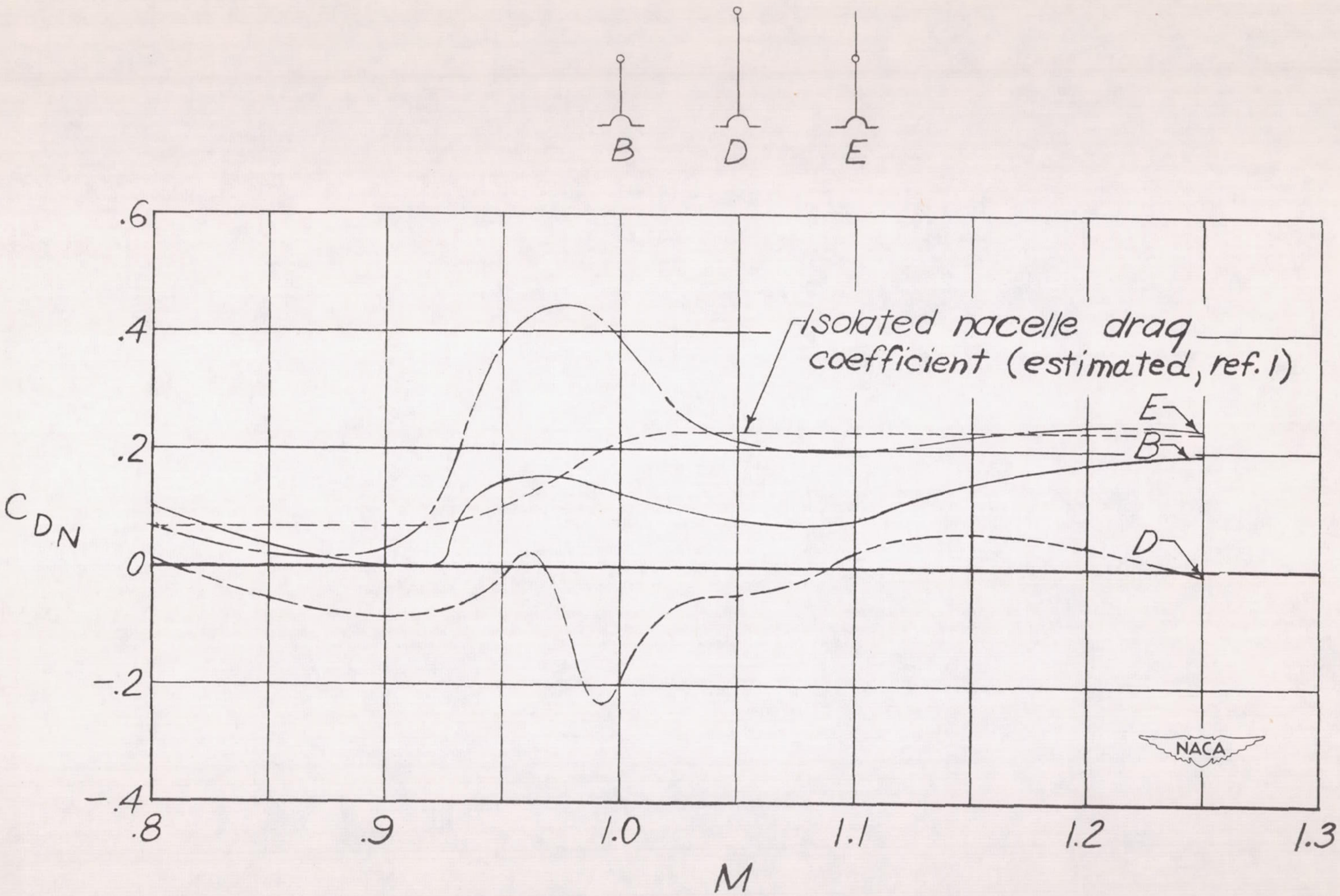


(c) Variation of nacelle-plus-interference drag coefficient with Mach number. $C_{D_N}$ based on nacelle frontal area.

Figure 7.- Concluded.